nature communications

Article

https://doi.org/10.1038/s41467-024-51827-3

A metabolic crosstalk between liposarcoma and muscle sustains tumor growth

Received: 17 February 2023

Accepted: 20 August 2024

Published online: 12 September 2024

Check for updates

Gabrielle Manteaux[1,9], Alix Amsel[1,9], Blanche Riquier-Morcant[1], Jaime Prieto Romero[1], Laurie Gayte[1], Benjamin Fourneaux[1], Marion Larroque[1], Nadège Gruel[2], Chloé Quignot[2], Gaelle Perot[3], Solenn Jacq[1], Madi Y. Cisse[1], Pascal Pomiès[4], Coralie Sengenes[5], Frédéric Chibon[3], Maud Heuillet[6,7], Floriant Bellvert[6,7], Sarah Watson[2,8], Sebastien Carrere[1], Nelly Firmin[1], Romain Riscal[1,10] ✉ & Laetitia K. Linares[1,10] ✉

Dedifferentiated and Well-differentiated liposarcoma are characterized by a systematic amplification of the *Murine Double Minute 2* (*MDM2*) oncogene. We demonstrate that p53-independent metabolic functions of chromatin-bound MDM2 are exacerbated in liposarcoma and mediate an addiction to serine metabolism to sustain tumor growth. However, the origin of exogenous serine remains unclear. Here, we show that elevated serine levels in mice harboring liposarcoma-patient derived xenograft, released by distant muscle is essential for liposarcoma cell survival. Repressing interleukine-6 expression, or treating liposarcoma cells with Food and Drugs Administration (FDA) approved anti-interleukine-6 monoclonal antibody, decreases de novo serine synthesis in muscle, impairs proliferation, and increases cell death in vitro and in vivo. This work reveals a metabolic crosstalk between muscle and liposarcoma tumor and identifies anti-interleukine-6 as a plausible treatment for liposarcoma patients.

Sarcomas, representing about 1% of all cancers, are malignant tumors of mesenchymal origin arising from soft or bone tissues. Among the 100 different histological subtypes of sarcomas, liposarcoma (LPS) represents the second most frequent subtype after gastrointestinal stromal tumors, accounting for 15–20% of all sarcomas[1]. The prognosis of LPS is highly heterogeneous, depending on the tumor location, its histological subtype, and the grade/size of the tumor at diagnosis[2–4]. Surgical resection performed in reference care centers remains the most efficient therapeutic strategy to date; however, the risk of recurrence and metastatic relapses varies between 20 to 40% in LPS patients, with a higher rate in patients with retroperitoneal tumors[5]. LPS is known to be poorly responsive to classical chemotherapies, including doxorubicin, ifosfamide, trabectedin, and eribulin[6]. Despite that, new targeted therapies, such as tyrosine kinase inhibitor Pazopanib, have demonstrated efficacy in patients with several types of sarcomas but showed no benefit in patients with LPS[7]. The median overall survival is estimated to be around 15 months[6,7], and the absence of treatment for metastatic or unresectable LPS reveals an urgent need for a novel therapeutic strategy for LPS. The most common LPS subtypes, well-differentiated and dedifferentiated LPS (WD-LPS and DD-

[1]IRCM, Institut de Recherche en Cancérologie de Montpellier, INSERM U1194, Université de Montpellier, Institut régional du Cancer de Montpellier, Montpellier, France. [2]INSERM U830, Diversity and Plasticity of Childhood Tumors Lab, PSL Research University, Institut Curie Research Center, Paris, France. [3]INSERM UMR 1037, Centre de Recherche en Cancérologie de Toulouse, Université Paul Sabatier Toulouse-III, Toulouse, France. [4]PhyMedExp, University of Montpellier-INSERM-CNRS, Montpellier, France. [5]RESTORE Research Center, Université de Toulouse, INSERM 1301, CNRS 5070, EFS, ENVT, Toulouse, France. [6]Toulouse Biotechnologie Institute (TBI), Université de Toulouse, CNRS, INRA, INSA, Toulouse, France. [7]MetaToul-MetaboHUB, National Infrastructure of Metabolomics and Fluxomics, Toulouse, France. [8]Department of Medical Oncology, Institut Curie Hospital, Paris, France. [9]These authors contributed equally: Gabrielle Manteaux, Alix Amsel. [10]These authors jointly supervised this work: Riscal Romain and Linares Laetitia K. ✉e-mail: romain.riscal@inserm.fr; laetitia.linares@inserm.fr

LPS, respectively), can typically coexist within the same tumor[8] and are characterized by the systematic amplification of the q13-15 region of chromosome 12, containing MDM2 in 100% of cases and CDK4 in 90% of cases. Apart from MDM2 amplification, previous studies have reported additional copy number alterations, such as *RB*, *JUN*, and *ASK1*[8,9]. The frequency of *Mdm2* amplification is such (almost 100%) that it is currently used for routine diagnosis to distinguish WD/DD-LPS from other sarcoma subtypes that commonly harbor p53 mutations[10,11].

The *mdm2* gene was first identified as the gene involved in the spontaneous transformation of an immortalized murine cell line, BALB/c 3T3. *Mdm2* was later labeled as an oncogene participating in cell transformation. *MDM2* encodes a well-characterized negative regulator of the p53 tumor suppressor. The MDM2 oncoprotein is frequently overexpressed in numerous human cancers[12] resulting in a loss of the tumor suppressor p53-dependent activities[13]. Under normal growth conditions, the p53 protein is kept at low levels by MDM2-mediated polyubiquitylation, inducing its degradation by the 26S proteasome. The role of MDM2 as a major regulator of p53 stability and transcriptional activities has been widely described by in vitro and in vivo models[13–15]. Through its E3 ligase activity, MDM2 affects the function of other cellular proteins involved in cell proliferation, DNA repair, ribosome biosynthesis, and many other processes that can also contribute to its oncogenic potential[16,17]. However, growing evidences suggest that MDM2 is involved in a complex network of protein interactions that confer MDM2 functions beyond its relationship with p53[18–21]. More recently, we started an in-depth analysis of MDM2 functions independently of p53 and demonstrated a key role in serine metabolism[22]. We have shown that MDM2 is recruited to chromatin (C-MDM2) in a p53-independent manner and regulates an ATF-3 and ATF-4-dependent transcriptional program. Although, we described that MDM2 is mainly recruited to chromatin under specific stress conditions such as oxidative stress. Moreover, performing a screen on a large panel of cancer cell lines, we identified dedifferentiated liposarcoma cell lines as the ones which consistently and spontaneously harbor C-MDM2[22,23]. The p53-independent metabolic functions of C-MDM2 are exacerbated in WD and DD-LPS and mediate an addiction to serine metabolism that sustains nucleotide synthesis, tumor growth and survival[23]. Despite several MDM2-p53 interaction-targeting molecules used in preclinical studies, success in the clinic has been limited[24,25]. Beyond the emergence of p53 alterations leading to drug resistance or treatment-related adverse events such as thrombocytopenia or neutropenia[26], we recently reported that the well-documented MDM2-p53 interaction inhibitor, Nutlin3-A, stabilizes p53 but unexpectedly enhances MDM2-mediated control of serine metabolism by increasing its recruitment to chromatin[23]. In contrast, genetic or pharmacological inhibition of C-MDM2 by SP141, a distinct MDM2 inhibitor triggering its degradation, and interfering with de novo serine synthesis, impaired LPS growth both in vitro and in clinically relevant patient-derived xenograft models. Taken together, our data suggest that targeting MDM2 functions in serine metabolism represents a potential therapeutic strategy for LPS[23,27].

The impact of cancer cells on their environment, locally and distantly, is known to promote malignancy and chemoresistance[28]. Understanding the interactions between cancer cell and surrounding metabolism will be critical for combining metabolism-targeted therapies with existing chemotherapies. It is known that cancer cells compete with cellular components of the microenvironment for essential nutrients, such as glucose, amino acids, and lipids. For example, restricting T cell glucose metabolism causes lymphocyte exhaustion[29], while high arginine levels promote enhanced T cell survival and anti-tumor activity[30,31]. The relationship between tumors and other organs is not limited to the immune system. Endothelial cells also undergo factor-induced metabolic reprogramming[32]. Cancer also causes alterations in whole-body metabolism that may influence how tumors access essential resources. Acting on nutrient availability through diet composition has been shown to slow cancer progression[33] and this field is likely to be a productive area of research in the near future.

In this study, we demonstrate a potential metabolic "long-distance" cooperation between normal tissues and LPS. Our data obtained in patient-derived mouse models of LPS (PDX) suggest that LPS somehow "educate" normal tissues/cells to support their massive demand for serine. While monitoring LPS growth in vivo, we observe an increase in circulating serine and glycine levels. Interestingly, skeletal muscles of these engrafted animals upregulate a transcriptional program involved in de novo serine synthesis, described to be regulated by C-MDM2 in cancer cells[23]. We hypothesize that metabolic cooperation between LPS cancer cells and surrounding muscle allows LPS tumors to maintain serine pools and now identify interleukin-6 (IL-6) as essential for LPS-mediated muscle reprogramming. Furthermore, blocking IL-6 using monoclonal antibodies, results in exogenous serine starvation in LPS cells and impaired proliferation in vitro and in vivo. As such, the exogenous serine provided by surrounding tissue, such as muscle, is critical for LPS tumor growth and reveals IL-6 as a plausible target for LPS treatments.

Results

Muscle reprogramming fuels Liposarcoma serine addiction

Recently, we classified liposarcoma as serine auxotroph[23]. To further investigate the significance of serine metabolism in liposarcoma models where *MDM2* and *CDK4* amplification were confirmed (Fig. 1A and Supplementary Fig. 1A–C), we examined circulating serine and glycine levels in nude mice xenografted with LPS cell lines or patient-derived mouse models (PDX). PDX are patient-derived tumor xenograft models generated by transferring freshly resected human tumor samples of primary naive LPS into immunodeficient nude mice. Surprisingly, we observed that circulating serine and glycine levels were significantly higher in mice harboring LPS tumors (PDXs and cell lines) relative to control mice (Fig. 1B–D and Supplementary Fig. 1D). Additionally, in response to MDM2 inhibitor treatment, which induces a drastic reduction in tumor growth[23], we were able to rescue serine and glycine levels to the baseline observed pre-engraftment, confirming a correlation between MDM2, circulating levels of serine and LPS tumorigenesis (Fig. 1B–D and Supplementary Fig. 1D). Given that more than 85% of the serine consumed by tumor cells comes from exogenous sources (Fig. 1E), we anticipated that liposarcoma tumors depend on serine synthetized by surrounding tissue. To test this hypothesis, we examined the expression of genes encoding limiting enzymes of the de novo serine synthesis pathway (SSP), including *3-phosphoglycerate dehydrogenase* (*Phgdh*), *phosphoserine aminotransferase 1* (*Psat1*), and *phosphoserine phosphatase* (*Psph*) in distant metabolic organs, such as the liver and muscles. Interestingly, these genes were upregulated in skeletal muscles of engrafted animals (Fig. 1F). In contrast, liver, kidney, brain and adipose tissue did not exhibit such activation of SSP genes (Fig. 1G and Supplementary Fig. 1E–G). These results indicate that muscle, and no other tissues, provides liposarcoma with serine and glycine amino acids. To further investigate the specificity of muscle-secreted serine on liposarcoma tumorigenesis, control mice fed with serine/glycine-deprived diet were analyzed. As expected, circulating serine and glycine levels were lower (Supplementary Fig. 1H), and SSP enzyme gene expression increased in the liver, known to be a major site for the de novo synthesis of serine[34] (Fig. 1H). Such an increase was not observed in other organs (Supplementary Fig. 1I–K), including muscle (Fig. 1I), confirming the specific serine metabolism rewiring in muscles from mice harboring LPS tumor. Furthermore, other tumor PDX models such as, leiomyosarcoma or breast cancer, failed to activate the de novo serine synthesis transcriptional program in vivo (Fig. 1J). Collectively, these results support a model in which the muscle-de novo serine synthesis transcriptional program is activated by liposarcoma tumor in vivo.

https://doi.org/10.1038/s41467-024-51827-3

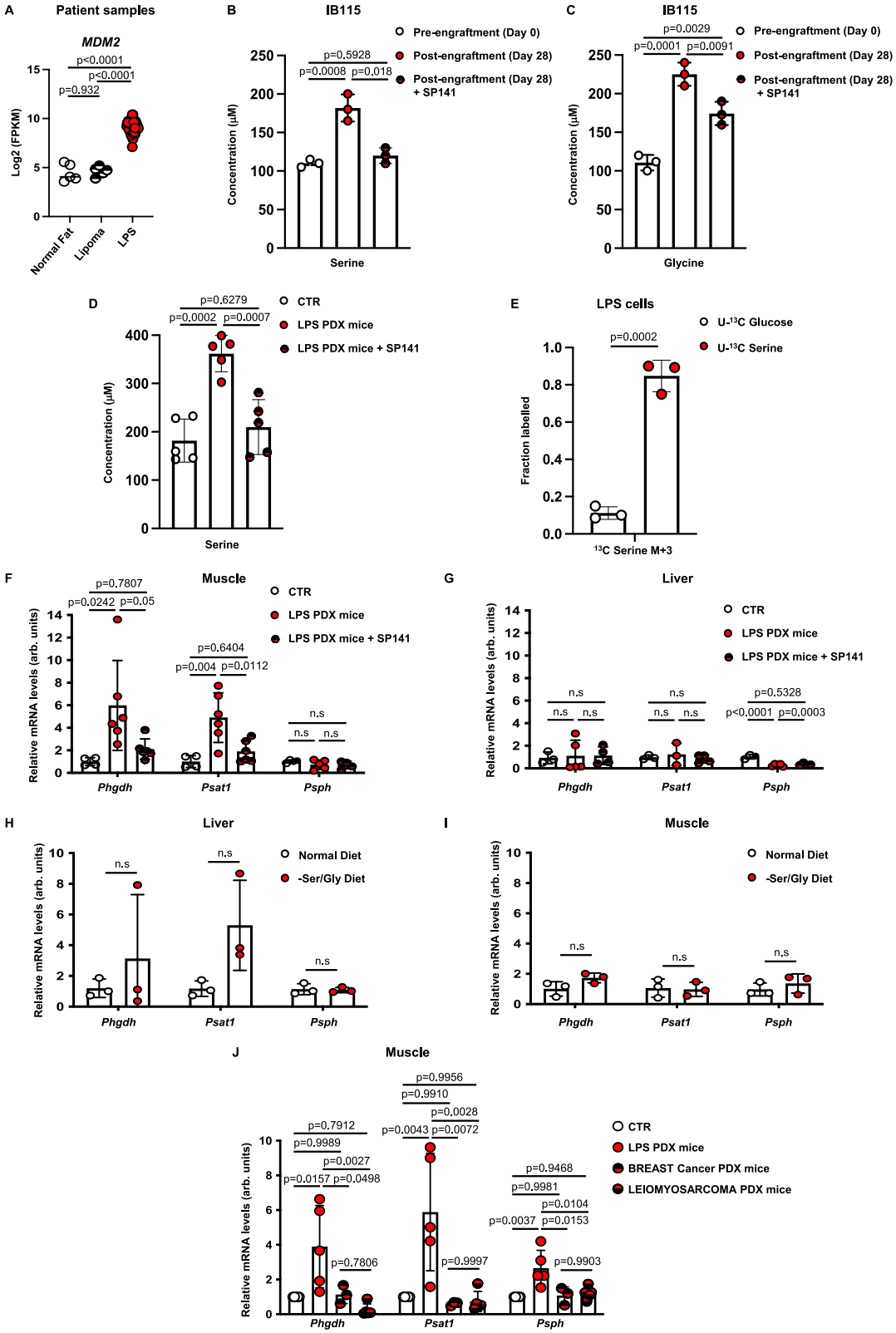

Liposarcoma cells take advantage of surrounding muscle cells for growth

To investigate the mechanisms by which liposarcoma cancer cells reprogram muscle cells, we developed in vitro models of co-culture with murine myoblast and human liposarcoma cell lines to assess mRNA levels of SSP enzymes. It should be noted that co-culture between human and murine cells allowed us to discriminate gene expression from the two population of cells present in the same dish using specific primers. Interestingly, C2C12 exhibit an increase of SSP genes expression in both contact and non-contact (T-W) co-culture experiments with LPS cells, whereas C2C12 cultured alone or with other cancer types, such as breast cancer (MCF7) or melanoma (A375) cell lines did not (Fig. 2A and Supplementary Fig. 2A–C). Our in vitro observations were also confirmed in transformed human myoblast

Fig. 1 | Liposarcoma reprogram serine synthesis pathway in muscles. **A** Normalized RNASeq reads of *MDM2*. (n = 5 normal fat tissues, 5 lipoma and 38 liposarcoma tumors). **B** Serine and **C** Glycine levels (µM) measured by HPLC, in nude mice before and 28 days post-engraftment of liposarcoma cells (IB115). Mice were treated daily with placebo or SP141 (40 mg/ml). ($n = 3$ experimental replicates). **D** Serine levels (µM) measured by HPLC. Control mice were compared to liposarcoma PDX Mice (LPS-PDX). Mice were treated daily with placebo or SP141 (40 mg/ml). ($n = 5$ animals/group). **E** Stable isotope tracing experiments in IB115 cells treated cultured for 48 h in the presence of uniformly labeled [U-13C]Glu and [U-13C]Ser in -Ser/Gly medium. LC-MS was used to detect the relative amount of the 13C-labeled m + 3 isotopolog of intracellular serine. ($n = 3$ experimental replicates). **F** Real-time qPCR analysis performed on LPS-PDX and control mice muscle, evaluating expression of serine synthesis pathway genes: *Phgdh, Psat1* and *Psph*. Mice were treated daily with placebo or SP141 (40 mg/ml). ($n = 6$ animals/group). **G** Real-time qPCR analysis performed on LPS-PDX and control mice liver, evaluating expression of serine synthesis pathway genes: *Phgdh, Psat1* and *Psph*. Mice were treated daily with placebo or SP141 (40 mg/ml). ($n = 5$ animals/group). **H** Real-time qPCR analysis performed control mice liver, evaluating expression of serine synthesis pathway genes: *Phgdh, Psat1* and *Psph*. Mice were fed with normal or -Ser/Gly diet. ($n = 3$ experimental replicates). **I** Real-time qPCR analysis performed on control mice muscle, evaluating expression of serine synthesis pathway genes: *Phgdh, Psat1* and *Psph*. Mice were fed with normal or -Ser/Gly diet. ($n = 3$ experimental replicates). **J** Real-time qPCR analysis performed on LPS-, Leiomyosarcoma- and Breast cancer-PDXs compared to control mice muscle, evaluating expression of serine synthesis pathway genes: *Phgdh, Psat1* and *Psph*. ($n = 5$ animals/group). Data are shown as means ± SEM and three or more independent experiments were performed. Statistical tests were all adjusted for multiple comparisons and included two-tailed unpaired t-test for (e, h, i), one-way analysis of variance (ANOVA) for a, b, c, d, f, g and j. $^{*}P < 0.05$, $^{**}P < 0.01$, $^{***}<0.001$, n.s = non-significant. Source data are provided as a Source Data file.

(Myo-E7) without affecting muscle differentiation states (Supplementary Fig. 2D, E). Moreover, to guarantee the exclusiveness of this special crosstalk between liposarcoma and muscle cells, liposarcoma cells were co-cultured with murine liver cells (BMEL). Compared to C2C12, SSP genes were not induced in BMEL cells (Fig. 2B). Additionally, suggesting that liposarcoma tumors could release factors leading to distant muscle metabolism rewiring, we collected culture media from LPS cells; conditioned media (CM). The media were conditioned 48 hours after LPS cells reached confluence, and 200µL of CM was added to 1,8 mL of fresh media, then compared to fresh media alone or fresh media complemented with CM from other cancer cell lines. Consistent with the increase of SSP genes observed in C2C12-LPS cells co-culture, treating C2C12 cells with CM from LPS cancer cell lines increased *Psat1, Phgdh and Psph* mRNA expression (Fig. 2C and Supplementary Fig. 2F). Similar results were obtained using myotubes (Supplementary Fig. 2G) and luciferase technology (Fig. 2D). A previous report from our lab demonstrated that an ATF4 dependent-C-MDM2 mechanism regulates the transcription of serine metabolism genes in LPS[23]. To investigate the potential functional roles of Mdm2 in our model, we employed murine shRNA to reduce Mdm2 expression in C2C12 cells (C2C12 sh*Mdm2*) (Supplementary Fig. 2H, I). The addition of IB115 in C2C12 sh*Scr* induced SSP genes expression, whereas IB115 failed to induce the same transcriptional program in sh*Mdm2* expressing C2C12 (Fig. 2E and Supplementary Fig. 2J). Moreover, depleting Mdm2 co-transcription factor, Atf4 by shRNA in C2C12 (C2C12 sh*Atf4*) (Supplementary Fig. 2K) also lead to similar results (Fig. 2F and Supplementary Fig. 2L) and suggests that the activation of the SSP transcriptional program LPS-mediated in C2C12 was Mdm2/Atf4 dependent. Interestingly, the increase of *Psat1, Phgdh and Psph* mRNA levels observed in C2C12 was associated with an increase of serine levels measured in the supernatant of LPS CM-activated C2C12 (Fig. 2G). In order to verify that the accumulation of serine was indeed generated by C2C12 cells specifically, we conducted co-culture experiments involving IB111 and C2C12 cells. Following 36 hours of activation, co-cultures were subsequently incubated with ^{13}C-labeled glucose for the indicated time point. Remarkably, we observed the presence of glucose-derived ^{13}C-labeled serine both intracellularly and in the culture media, indicating that the observed increase in serine, which fed the LPS cells, is directly linked to serine production originated from muscle cells (Fig. 2H, I). Moreover, to validate that liposarcoma cells rely on muscle serine production for growth, LPS cells were cultured in media without serine and glycine (-Ser/Gly) and supplemented or not with C2C12 cells. We observed proliferation defects in the absence of serine and glycine compared to cells grown in complete media. Interestingly, co-culturing LPS cells with C2C12 in -Ser/Gly, fully rescued LPS cells proliferation (Fig. 2J). These data were also confirmed using CM from LPS-activated C2C12, while CM from HPAC-activated C2C12 did not rescue proliferation defect of IB115 grown in media without serine and glycine (Fig. 2K and Supplementary Fig. 2M, N). Similar results were obtained using human myoblast (Supplementary Fig. 3A). Additionally, SSP proteins (Fig. 2L) and mRNAs (Fig. 2C) expression were similarly increased in C2C12 exposed to IB115 CM. Lately, we investigated whether C2C12 SSP enzymes were required to rescue IB115 proliferation by generating C2C12 sh*Psat1* and sh*Phgdh* (Supplementary Fig. 3B-E). C2C12 sh*Psat1* or sh*Phgdh* were unable to rescue IB115 proliferation (Fig. 2M), indicating that C2C12 SSP machinery is required to promote LPS proliferation. Furthermore, SSP genes have been shown to be regulated at the epigenetic level through methylation of histone H3 on lysine 9 (H3K9)[22,35,36]. Interestingly, the presence of IB111 CM resulted in an increased level of the activation mark mono-methylation of H3K9 (H3K9Me1) in C2C12 cells (Supplementary Fig. 3F). Subsequently, we assessed the impact of LPS CM on the NAD+/NADH ratio known to be related to PHGDH activity. In C2C12 cells, the addition of CM led to an increase in the NAD+/NADH ratio (Supplementary Fig. 3G). Collectively, our data indicate that the association between LPS cells and muscle cells is required to sustain serine levels and the proliferation of LPS cells in an MDM2-dependent manner.

Liposarcoma-released IL-6 regulates muscle reprogramming

We hypothesized that LPS cells might acquire functions, such as secreting factors able to induce serine metabolism in distant muscle. To determine the implicated secreted factors, we collected LPS cells-grown media. The analysis of this culture supernatant using a cytokines array showed that LPS cells release different cytokines, including interleukin-6 (IL-6) (Fig. 3A). Beside its role in immunity, previous reports linked IL-6 expression with ATF4 in macrophages[37,38]. Furthermore, MDM2 has been involved in a IL-6-mediated degradation of p53[39]. For those reasons, we decided to explore further the role of IL-6 in the crosstalk between LPS and muscle. In order to confirm this result, we examined *IL-6* gene expression in IB115 and IB111 liposarcoma cell lines relative to other cancer cell lines and observed higher *IL-6* mRNA levels in LPS cell lines (Fig. 3B). IL-6 protein levels were also higher in supernatant of liposarcoma cell lines analyzed by ELISA (Fig. 3C). Additionally, to determine whether IB115-released IL-6 could play a significant role in proliferation, we treated IL-6-dependent myeloma cell line XG-6 with IB115 CM. While recombinant IL-6 and CM from IB115 were able to support XG-6 proliferation, CM from MCF7 did not (Fig. 3D). To further investigate the molecular mechanism by which IL-6 is released from LPS tumors, we performed ChIP experiments on IB115 cells. We observed ATF4 and MDM2 binding on the *IL-6* promoter (Fig. 3E), suggesting that ATF4/MDM2 complex is involved in *IL-6* transcription in LPS cells. Furthermore, we confirmed IL-6 regulation through ATF4 and MDM2 in LPS cells using shRNA technology. IB115 sh*MDM2* or sh*ATF4* resulted in decrease *IL-6* mRNA levels and IL-6-

https://doi.org/10.1038/s41467-024-51827-3

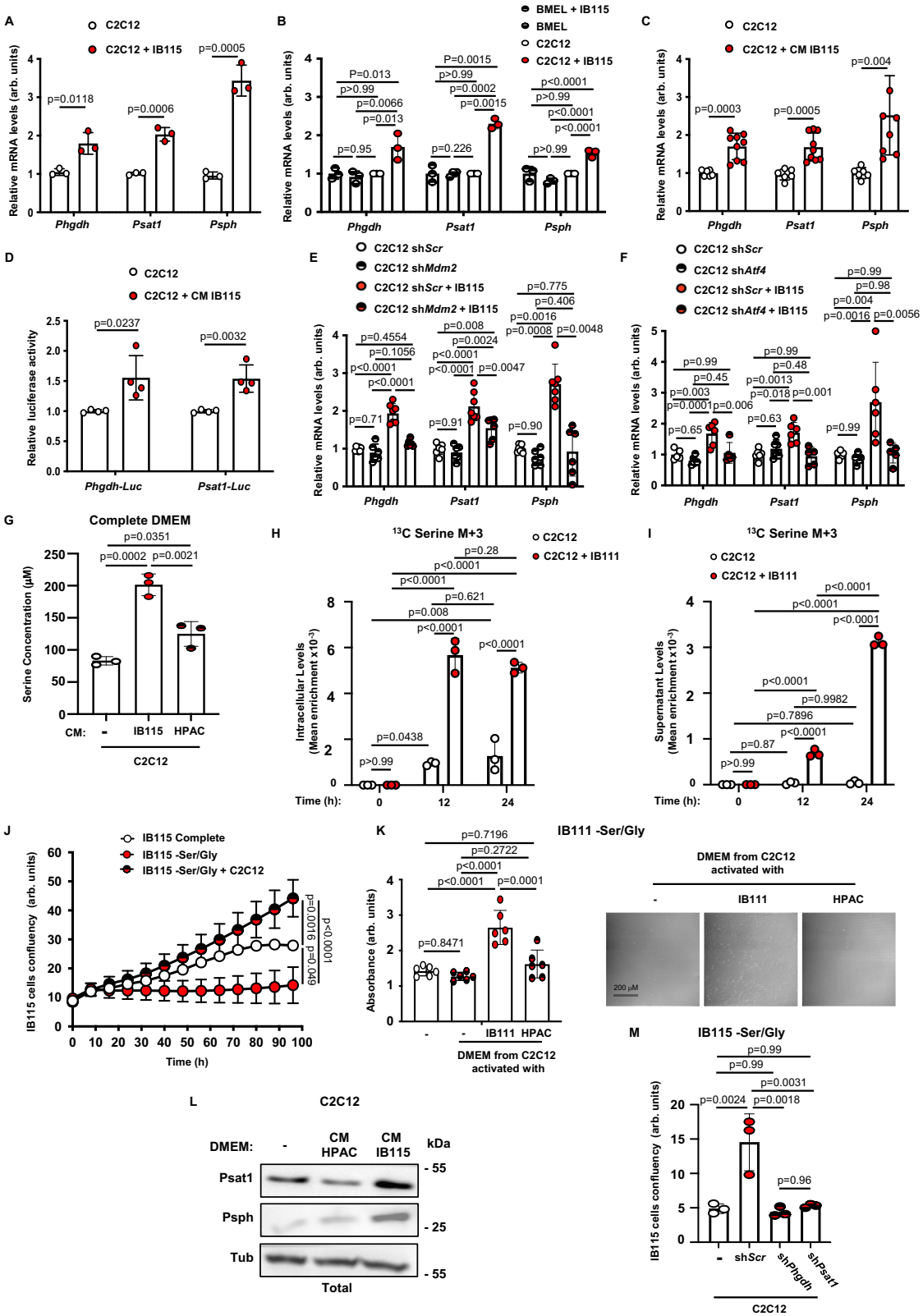

excreted protein from LPS cells to the same degree as sh*IL-6* did (Fig. 3F, G and Supplementary Fig. 4A, B). To determine the role of IL-6 on muscle reprogramming, we analyzed the level of SSP genes in C2C12 murine myoblast cultured in the presence of recombinant IL-6. Interestingly, 50 pg/ml of IL-6 were sufficient to activate serine synthesis genes expression in C2C12 (Fig. 3H). These results were also confirmed by targeting actors of the IL-6 pathway in LPS and muscle cells. Interestingly, the serine transcriptional program mediated by IL-6 was not observed in C2C12 cells when depleted of IL-6 receptor (C2C12 sh*IL-6Rα*) or cocultured with IB115 sh*IL-6* (Fig. 3J, K and Supplementary Fig. 4C–F). Collectively, these results showed that LPS cells-released IL-6 promotes serine metabolism reprogramming in muscle cells, which, in turn, provides serine to sustain LPS cells proliferation.

Fig. 2 | Liposarcoma needs muscle reprogramming to sustain proliferation. **A** Real-time qPCR analysis performed on C2C12 cocultured with IB115 cells (ratio 1:2), evaluating expression of serine synthesis pathway genes: *Phgdh, Psat1*, and *Psph*. ($n = 3$ experimental replicates). **B** Real-time qPCR analysis performed on C2C12 or BMEL murine cells cocultured with IB115 cells (ratio 1:2), evaluating expression of serine synthesis pathway genes: *Phgdh, Psat1*, and *Psph*. ($n = 3$ experimental replicates). **C** Real-time qPCR analysis performed on C2C12 cells incubated 16 h with IB115 conditioned media, evaluating the expression of serine synthesis pathway genes: *Phgdh, Psat1* and *Psph*. ($n = 9$ experimental replicates). **D** Luciferase assay performed on C2C12 cells incubated 16 h with IB115 conditioned media, evaluating relative luciferase activity of *Phgdh* and *Psat1* reporter. ($n = 4$ experimental replicates). **E** Real-time qPCR analysis performed on C2C12 cells after sh*Scr* or sh*Mdm2* cocultured with IB115 cells (ratio 1:2), evaluating the expression of serine synthesis pathway genes: *Phgdh, Psat1* and *Psph*. ($n = 8$ experimental replicates). **F** Real-time qPCR analysis performed on C2C12 cells after sh*Scr* or sh*Atf4* cocultured with IB115 cells (ratio 1:2), evaluating the expression of serine synthesis pathway genes: *Phgdh, Psat1*, and *Psph*. ($n = 6$ experimental replicates). **G** Serine levels (µM) measured by HPLC in C2C12 grown in Complete DMEM alone or incubated with IB115 or HPAC CM. (n = 3 experimental replicates). **H** Stable isotope tracing experiments performed in C2C12 cells cocultured with IB111 for 36 hours. Then, cells were cultured for the last 12 or 24 hours in the presence of uniformly labeled [U-13C]Glu. LC-MS was used to detect the mean enrichments of ^{13}C-labeled (m + 3) isotopologs detected in intracellular serine that derive from ^{13}C-labeled glucose. ($n = 3$ experimental replicates). **I** Stable isotope tracing experiments performed in C2C12 cells cocultured with IB111 for 36 hours. Then, cells were cultured for the last 12 or 24 hours in the presence of uniformly labeled [U-13C]Glu. LC-MS was used to detect the mean enrichments of ^{13}C-labeled (m + 3) isotopologs detected in extracellular serine that derive from ^{13}C-labeled glucose. ($n = 3$ experimental replicates). **J** Proliferation assay was performed on IB115 cells grown in media supplemented with or without Serine and Glycine and cocultured with C2C12 cells. ($n = 3$ experimental replicates). **K** Crystal violet quantification and representative photographs of IB111 cells grown in media without Serine and Glycine and supplemented with C2C12 or HPAC CM for 5 days. ($n = 6$ experimental replicates). **L** Psat1 and Psph protein expression assessed by immunoblot in C2C12 supplemented or not with IB115 or HPAC CM. Tubulin was used as the loading control. **M** End point of proliferation assay performed on IB115 cells grown in media without Serine and Glycine and cocultured with C2C12 cells after sh*Scr*, sh*Phgdh*, or sh*Psat1* knockdown. ($n = 3$ experimental replicates). Data are shown as means ± SEM and three or more independent experiments were performed. Statistical tests were all adjusted for multiple comparisons and included two-tailed unpaired *t*-test for (a, c, d), one-way (b, e, f, g, k, m), and two-way analysis of variance (ANOVA) for h, i and j. $^{*}P < 0.05$, $^{**}P < 0.01$, $^{***}<0.001$, n.s = non-significant. Source data are provided as a Source Data file.

Targeting the IL-6/STAT3 pathway impairs serine biosynthesis activation in reprogrammed muscle cells

IL-6 is involved in various physiological and pathological processes, including immune response, inflammation, and regulation of certain cellular activities such as metabolism[40]. Several strategies can be employed to target IL-6, with IL-6 monoclonal antibodies designed to specifically bind to IL-6 or its receptor being the main successful approaches in the treatment of certain inflammatory and autoimmune disorders[31]. We focused on IL-6 antibodies (BE8, hBE8, Siltuximab) treatment on C2C12 co-cultured with serine-deprived LPS cells. Interestingly, targeting IL-6 with three different antibodies, blocked de novo serine synthesis enzymes expression in C2C12 compared to vehicle-treated cells (Fig. 4A, B and Supplementary Fig. 5 A-C). Importantly, LPS cells exhibited proliferation defects, phenocopying the effects of targeting serine synthesis enzymes in C2C12 and confirming the importance of IL-6 to induce de novo serine transcriptional program in C2C12 (Fig. 4C). Of note, LPS cells did not increase de novo serine synthesis machinery to provide substrate for proliferation, confirming the LPS auxotrophy for muscle-released serine (Supplementary Fig. 5D). Moreover, IL-6-targeted co-culture exhibited elevated cell death in vitro (Supplementary Fig. 5E). Similar results were observed with bazedoxifene (BZA), drug-targeting GP130 (IL-6Rα) (Fig. 4D and Supplementary Fig. 5F). Serine metabolism readouts were also verified after IL-6 addition in C2C12 cells (Fig. 4E, F). Mechanistically, the Janus kinase-signal transducer and activator of transcription (JAK-STAT) pathway is one of the key signaling pathways through which IL-6 exerts its effects[41]. We hypothesized that JAK/STAT3 signaling pathway could play a prominent role in mediating effects of IL-6 on muscle reprogramming, and that our observed IL-6-dependent proliferation phenotype was at least partially mediated through STAT3 signaling pathway in C2C12. STAT3 phosphorylation was increased in C2C12 stimulated with recombinant IL-6 or IB115 CM (Fig.4G) while HPAC CM did not. Treatment with STAT3 inhibitors also led to serine metabolism transcriptional program and LPS proliferation defects (Fig. 4H, I and Supplementary Fig. 5G, H). Published data from our lab and others have shown interesting links between ATF4/MDM2[22] and ATF4/STAT3[42] suggesting that JAK/STAT3 signaling pathway could play a prominent role in mediating effects of IL-6 on muscle reprogramming. Therefore, how STAT3 is connected to MDM2/ATF4 to induce serine biosynthesis will require more investigation in the future. Taken together, our data suggest that LPS-released IL-6 appears to be critical to sustain STAT3 signaling and control muscle reprogramming. Blocking LPS-muscle crosstalk through IL-6 inhibitors and/or serine restriction could offer a potential combination therapy for patients with liposarcoma.

Alternative therapeutic opportunity in liposarcoma

Our findings demonstrate the importance of the IL-6/STAT3/Serine axis for liposarcoma carcinogenesis and identify immunotherapy using IL-6 antibody as a promising treatment in liposarcoma therapy. To assess the clinical and in vivo relevance of our findings, we initially measured circulating IL-6 levels in mice harboring PDXs relative to normal mice. ELISA analysis revealed higher circulating IL-6 levels in LPS-PDX mice compared to leiomyosarcoma or breast cancer PDXs (Fig. 5A). Additionally, we examined *IL-6* mRNA expression in different sarcoma subtypes. Interestingly, this analysis of primary human LPS tumors compared to other sarcoma subtypes revealed a significant accumulation of *IL-6* mRNA levels in LPS tumors (Fig. 5B). Furthermore, independent gene expression analysis of human LPS clinical samples and cell lines (DepMap) compared to other tumor types revealed significant increase of *IL-6* mRNA levels (Supplementary Fig 6A, B), confirming that IL-6 expression is a particular characteristic of liposarcoma. To assess the in vivo relevance of IL-6 pathway blockade, we assessed the effect of Siltuximab (monoclonal antibody) or doxorubicin (first-line treatment for primary LPS) on xenograft tumor derived from LPS cell lines and PDX-LPS. Siltuximab treatment decreased tumor growth without visible side effect, whereas doxorubicin had no statistically significant effect (Fig. 5C, D and Supplementary Fig. 6C). Siltuximab-treated mice exhibited reduced circulating serine and reduced IL6 expression (Fig. 5D, E and Supplementary Fig. 6D–F).

Given that liposarcoma tumor are diet- and muscle-serine auxotrophs, we treated LPS-PDX mice with anti-IL-6 (BE8) while fed with either a serine/glycine-free or normal diet to evaluate the therapeutic use of our findings. Mice receiving the combination of deprived serine diet and anti-IL-6 treatment exhibited reduced tumor growth compared to mice receiving a normal diet and vehicle (Fig. 5F and Supplementary Fig. 6G). As validated by IHC, anti-IL-6-treated tumors exhibited reduced tumor proliferation and elevated cell death as indicated by Ki67 and cleaved caspase 3 staining (Supplementary Fig. 7A, B). These data support the notion that serine/glycine metabolism initiated in muscle by LPS tumors is a driving event to sustain LPS tumor growth.

Furthermore, we initiated a collaboration with clinicians of the 'Institut du Cancer de Montpellier' (ICM), allowing us to generate a

https://doi.org/10.1038/s41467-024-51827-3

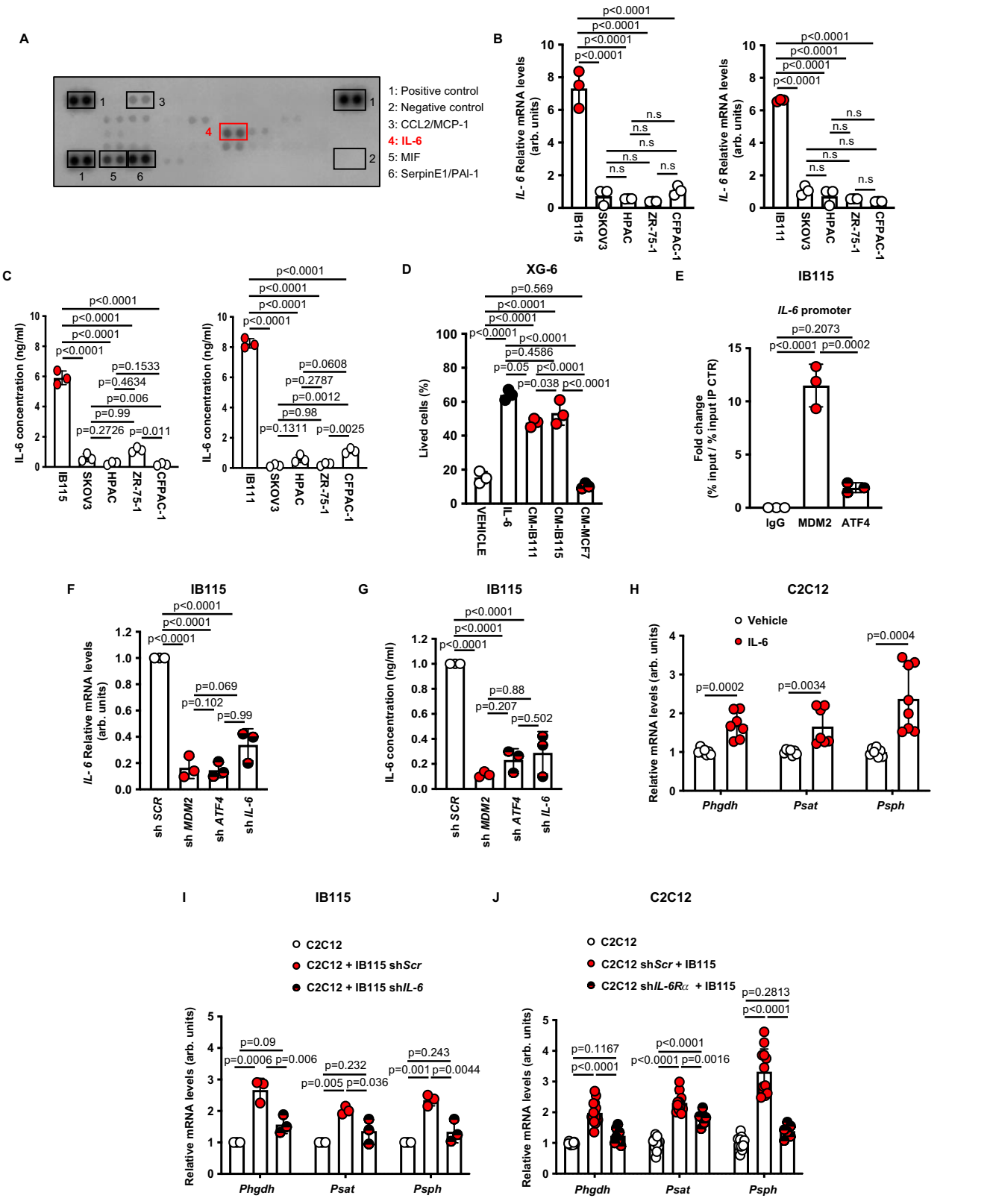

clinical-biobank (BCB) regrouping a collection of fresh tumors and blood samples from LPS and other sarcoma patients. Using this biobank, we conducted a preliminary study on a small cohort and noticed that circulating serine levels significantly decreased after that LPS tumor was removed by surgery (Fig. 5G, H and Supplementary Fig. 7C, D). Of note, serine levels did not change after surgery in other sarcoma subtypes including UPS (Fig. 5I and Supplementary Fig. 7E and Supplementary Tables 2 and 3). Interestingly, few patients showed early recurrence and surprisingly, when looking at their circulating serine profile, we noticed that serine levels did not drop as observed in other patients (Fig. 5G and Supplementary Fig. 7C, D). In aggregate, our findings demonstrate that LPS cells are dependent on exogenous serine released by IL-6-activated muscle. Either genetic or pharmacological inhibition of IL-6 decreased circulating serine and inhibited LPS

Fig. 3 | Liposarcoma-released IL-6 reprograms distant muscles. A Proteome Profiler Human Cytokine Array. **B** Real-time qPCR analysis of *IL-6* mRNA level of different cancer cell lines, SKOV3, HPAC, ZR-75.1, CFPAC-1, including LPS cell lines, IB115 and IB111. ($n = 3$ experimental replicates). **C** IL6 concentration (ng/ml), measured by ELISA, of different cancer cell lines, SKOV3, HPAC, ZR-75.1, CFPAC-1, including LPS cell lines, IB115 and IB111. ($n = 3$ experimental replicates). **D** End point of proliferation assay performed on XG-6 cells grown in media supplemented with the vehicle, recombinant IL-6, IB115, IB111, or MCF7 conditioned media. ($n = 3$ experimental replicates). **E** qChIP experiments showing the relative amounts of MDM2 and ATF4 on the *IL-6* promoter in IB115 cells. Results were represented as the relative ratio between the mean value of immunoprecipitated chromatin (calculated as a percentage of the input) with the indicated antibodies and one control irrelevant antibody. ($n = 3$ experimental replicates). **F** Real-time qPCR analysis of *IL-6* mRNA level in IB115 cells after sh*Scr*, sh*Mdm2*, sh*Atf4 or* sh*IL-6* lentiviral infection, puromycin selection (48 h, 2µg/mL). ($n = 3$ experimental replicates). **G** IL6 concentration (ng/ml), measured by ELISA, of IB115 cells after sh*Scr*, sh*Mdm2*, sh*Atf4 or* sh*IL-6* lentiviral infection, puromycin selection (48 h, 2µg/mL). ($n = 3$ experimental replicates). **H** Real-time qPCR analysis performed on C2C12 cells grown in media supplemented with vehicle or recombinant IL6 (50 pg/mL), evaluating the expression of serine synthesis pathway genes: *Phgdh, Psat1*, and *Psph*. (n = 8 experimental replicates). **I**, Real-time qPCR analysis performed on IB115 cells after sh*Scr* or sh*IL-6* cocultured with C2C12 cells (ratio 1:2), evaluating the expression of serine synthesis pathway genes: *Phgdh, Psat1*, and *Psph*. ($n = 3$ experimental replicates). **J**, Real-time qPCR analysis performed on C2C12 cells after sh*Scr* or sh*IL-6Rα* cocultured with IB115 cells (ratio 1:2), evaluating the expression of serine synthesis pathway genes: *Phgdh, Psat1*, and *Psph*. ($n = 13$ experimental replicates). Data are shown as means ± SEM and three or more independent experiments were performed. Statistical tests were all adjusted for multiple comparisons and included two-tailed unpaired t-test for (h), one-way analysis of variance (ANOVA) for b, c, d, e, f, g, I, and j. $^{*}P < 0.05$, $^{**}P < 0.01$, $^{***}<0.001$, n.s non-significant. Source data are provided as a Source Data file.

proliferation (Fig. 5J). These data suggest that screening for serine levels in liposarcoma patient undergoing surgery could be further developed to predict potential recurrences and that compounds specifically targeting IL-6, its receptor or downstream effectors, either singly or in combination with a restricted serine regiment, could be further addressed as an alternative therapeutic strategy to treat liposarcoma patients.

Discussion

WD- and DD-LPS, the most frequent LPS subtypes, are poorly responsive to classical chemotherapies, and there is currently no cure available for metastatic or unresectable LPS. The first-line treatment for LPS is surgery and high doses of doxorubicin could be administered, but it provides limited clinical benefit and commonly results in severe side effects[43]. We recently demonstrated that, in contrast to other types of sarcoma, all LPS display constitutive recruitment of C-MDM2 and are highly dependent on exogenous serine[23]. In mammals, serine is considered as a nonessential amino acid, the majority of which is synthesized de novo from glycolysis. Interestingly, many tumors such as triple-negative breast cancer and melanoma upregulate PHGDH expression leading to SSP flux increase and tumor growth in vivo[44,45]. However, other tumors such as liposarcoma and lung cancer depend on the availability of extracellular serine suggesting that serine needs vary among cancer types[46].

Nevertheless, liposarcoma cells consume large amounts of extracellular serine regardless of SSP activity and could affect exogenous serine availability. Counterintuitively, we observed that patients and PDX mice with liposarcoma exhibit high levels of circulating serine in blood compared to control mice fed with the same diet. We show here that muscles provide extracellular serine to sustain liposarcoma proliferation. Generating LPS-PDXs mice, which increased serum serine levels, demonstrates that de novo serine synthesis machinery was activated in these mice muscles. This was surprising, due to the distance between muscle and tumor, but muscles have already been described as a signaling organ releasing cytokines and metabolites during exercise. Moreover, skeletal muscle comprises various fiber types with specific functions tailored to different tasks. We hypothesized that those composed specifically of glycolytic fibers (type IIb and IIx), associated with performance in high-velocity and short-duration activities, could be those showing an elevation in serine synthesis. More work should be done to confirm this hypothesis. In terms of our study's utilization of primary muscle myoblasts versus undifferentiated C2C12 cells, we would like to provide further clarification. We acknowledge that relying predominantly on undifferentiated C2C12 cells may pose a limitation to our research. While these cells offer advantages in terms of experimental tractability and reproducibility, they may not fully capture the complexity of in vivo muscle physiology. However, it's worth noting that certain experiments were conducted using differentiated C2C12 cells, as well as muscle tissue sampled in vivo including major cell types composing the myofiber microenvironment. Our findings strongly indicate that myofibers are the primary source of serine released from muscle tissue.

Taken together, our data reveal that conditioned media from proliferating LPS cells was sufficient to increase serine synthesis genes in muscle murine cell lines.

The underlying signaling events linking LPS proliferation and muscle serine metabolism are likely to be complex, but previous studies revealed that tumorkines are intimately involved in the initiation and progression of cancer, and circulating levels of many tumorkines are elevated in diverse cancer types. We found that IL-6 expression and concentration were elevated in LPS tumors compared to other cancer types tested. Using functional in vitro and in vivo studies, we demonstrate that LPS cells establish a metabolic cooperation with normal surrounding muscles to sustain serine requirements via IL-6 release. We observed that, using IL-6 pathways, LPS have the amazing power to reprogram distant muscles. Thus, understanding tumor biology beyond their own metabolic regulation seems to be essential to develop new therapeutic strategies. The molecular basis of increased IL-6 expression is mediated through MDM2/ATF4 chromatin function involved in serine homeostasis in LPS cells. As for MDM2, we provide genetic and pharmacological evidence that targeting IL-6-associated metabolic functions represents an efficient alternative strategy for treating LPS.

IL-6 is a cytokine that plays roles in immunity, tissue regeneration, and metabolism. The production of IL-6 contributes to the defense during infection, but dysregulation of IL-6 signaling is also involved in disease pathology. The biological role of IL-6 has been implicated in various autoimmune diseases such as rheumatoid arthritis and some other acute and chronic inflammations[47]. In addition to its critical role in several diseases, IL-6 has very recently been reported key in the pathogenesis of multicentric Castleman disease (MCD)[38]. These features and our data make IL-6 and IL6-Rα attractive therapeutic targets, leading to the development of IL-6 pathway inhibitors including siltuximab, which has been granted full approval by the Food and Drug Administration (FDA). In addition to our in vitro and in vivo experiments using siltuximab, further studies will be required to assess the efficacy and clinical utility of repurposing Siltuximab for liposarcoma therapy. Finally, our work highlights clearly the intriguing and emerging metabolic field of tumor-organ communication and may also suggest alternative combination therapies.

Methods

Ethical Statements

All the cell lines and constructs used for in vitro experiments were registered by the French "MINISTERE DE L'ENSEIGNEMENT SUPERIEUR, DE LA RECHERCHE ET DE L'INNOVATION" (DUO N°11558).

https://doi.org/10.1038/s41467-024-51827-3

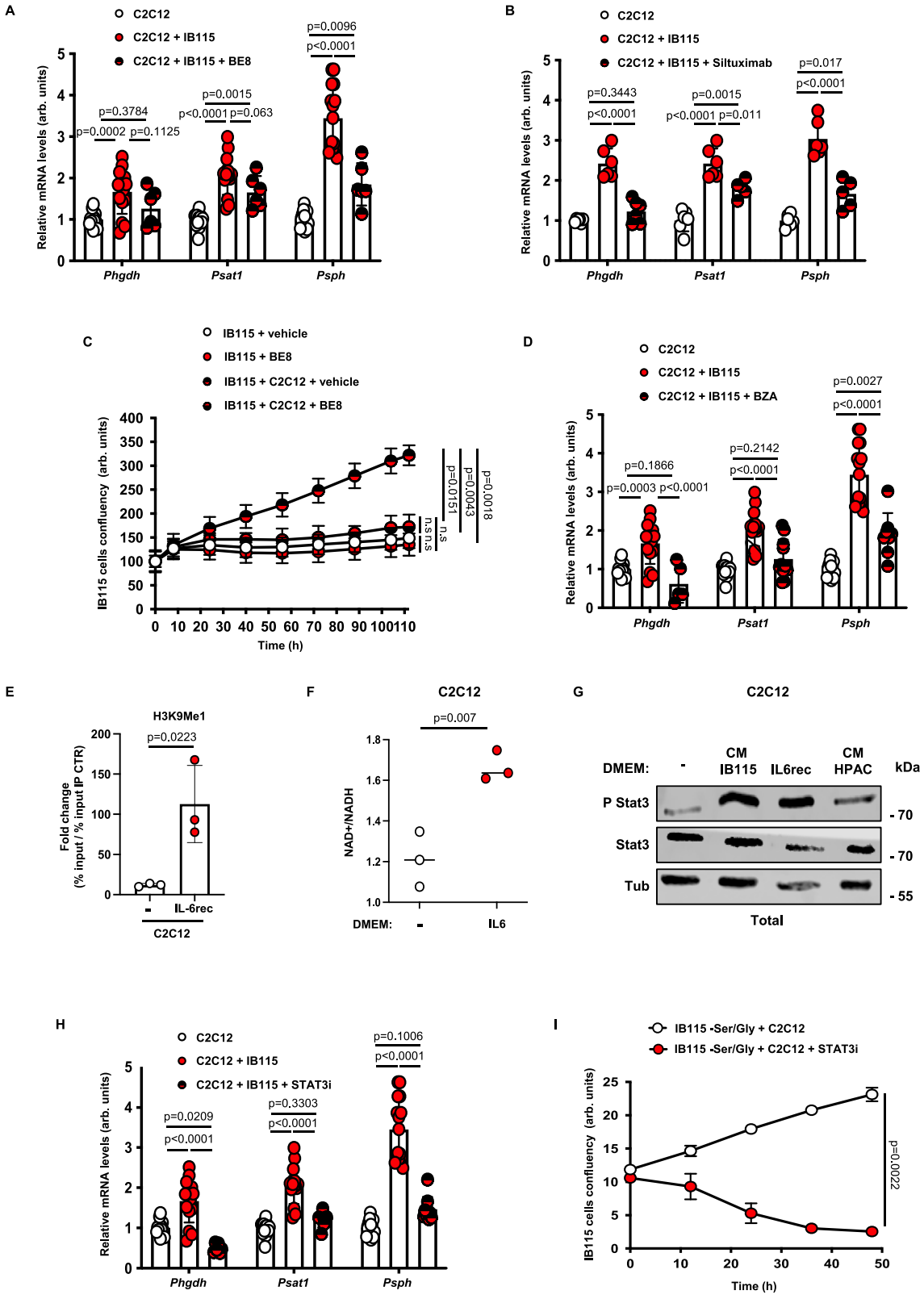

All animal procedures were evaluated by the ethic committee for animal warfare of the region Languedoc Roussillon (Comité d'Ethique en Expérimentation Animal Languedoc Roussillon, CEEALR36) and approved by "MINISTERE DE L'ENSEIGNEMENT SUPERIEUR, DE LA RECHERCHE ET DE L'INNOVATION" (structure agreement numbers # E 34-172-27 and project agreement # 2021011115238381-#28923). Animal housing and euthanasia were performed in accordance with the 3R rule and with recommendations of the Guide for the Care and Use of Laboratory Animals.

Human samples were obtained from patients with histologically confirmed sarcoma upon validation by board-certified pathologists. Samples were included in our clinical biobank after the written agreement of patients and approval by the local Ethics Committee and the National Agency for Drug Safety (Agence Nationale de Sécurité du

Fig. 4 | Targeting IL-6/STAT3 pathway impairs liposarcoma proliferation. Real-time qPCR analysis performed on C2C12 cells alone or cocultured with IB115 cells supplemented with vehicle, anti IL-6 (BE8) **A**, or Siltuximab **B**, evaluating expression of serine synthesis pathway genes: *Phgdh, Psat1* and *Psph*. (A $n = 15$, B $n = 6$, experimental replicates). **C**, Proliferation assay performed on IB115 cells alone or cocultured with C2C12 cells grown in media without Serine and Glycine and supplemented with vehicle or anti IL-6 (BE8). ($n = 3$ experimental replicates). **D**, Real-time qPCR analysis performed on C2C12 cells alone or cocultured with IB115 cells supplemented with vehicle or GP130 inhibitor (BZA), evaluating expression of serine synthesis pathway genes: *Phgdh, Psat1* and *Psph*. ($n = 15$ experimental replicates). **E** qChIP experiments showing the relative amounts of mono-methylation of lysine 9 of histone H3 (H3K9Me1) on the *Psat1* promoter in C2C12 treated or not with recombinant IL-6. Results were represented as the relative ratio between the mean value of immunoprecipitated chromatin (calculated as a percentage of the input) with the indicated antibodies and a control irrelevant antibody. ($n = 3$ experimental replicates). **F** NAD+/NADH ratio in C2C12 treated or not with recombinant IL-6. ($n = 3$ experimental replicates). **G** STAT3, and P-STAT3 protein expression assessed by immunoblot in C2C12 cells incubated 16 h with recombinant IL-6, IB115, or HPAC conditioned media. Tubulin was used as the loading control. **H** Real-time qPCR analysis performed on C2C12 cells alone or cocultured with IB115 cells (ratio 1:2) supplemented with vehicle or STAT3 inhibitor, evaluating expression of serine synthesis pathway genes: *Phgdh, Psat1*, and *Psph*. ($n = 15$ experimental replicates). **I** Proliferation assay performed on IB115 cells grown in media without Serine and Glycine and cocultured with C2C12 cells treated or not with STAT3 inhibitor. ($n = 3$ experimental replicates). Data are shown as means ± SEM and three or more independent experiments were performed. Statistical tests were all adjusted for multiple comparisons and included two-tailed unpaired t-test for (e, f), one-way (a, b, d, h) and two-way analysis of variance (ANOVA) for c and i. $^{*}P < 0.05$, $^{**}P < 0.01$, $^{***}<0.001$, n.s. non-significant. Source data are provided as a Source Data file.

Médicament (ANSM); ANSM number: 2016-A00638-43 and CRB-ICM agreement BB-033-0059).

Reagents. Recombinant Human IL-6 protein, Bazedoxifène, C188-9, Stattic, Phosphatase inhibitor cocktail 2, all unlabeled amino acids, formic acid (98% LC-MS grade), acetonitrile (>99.9% LC-MS grade), and methanol (>99.9% LC-MS grade) were purchased from Sigma-Aldrich. Protease inhibitor complete EDTA-free was purchased from Roche. The MDM2 inhibitor SP141 was synthesized based on the published structure[1]. Siltuximab (SYLVANT®) and Tocilizumab were purchased at the "ICM" pharmacy. Elsilimomab (BE8) et mAB 1339 (humanized αIl-6) were purchased from Evitria.

Cell culture. Cell lines used in this study were ordered at ATCC:

C2C12 N°CRL-1772, HPAC N°CRL-2119, SKOV3 N°HTB-77, ZR-75.1N°CRL-1500, CFPAC.1N°CRL-1918. Authentication was done by Eurofins and presented in supplementary data. IB115 and IB111 are homemade cell lines provided by F. Chibon. Authentication as liposarcoma cell lines were verified by CGH and FISH during the study (supplementary Fig. 8).

XG6 Myeloma Cell Line (HMCL) was authenticated according to their short tandem repeat profiling. Affymetrix U133 plus 2.0 microarrays data have been deposited in the ArrayExpress public database under accession numbers ETABM-937 and E-TABM-1088 (Alaterre E at al. Theranostics 2022).

All cell lines were weekly tested for mycoplasma with MycoAlert® Mycoplasma Detection Kit (Lonza).

Unless otherwise stated, cell culture reagents were purchased from Gibco (Invitrogen). Cells were kept at 37 °C in a humidified 5% CO_2 incubator and maintained in DMEM Glutamax supplemented with 10% FBS (Hyclone, Thermo Scientific) and 1% Penicilline/Streptavidin. For Serine and Glycine starvation proliferation experiments, cells were cultured in DMEM lacking amino acids supplemented with 1% Dialysed serum (Sigma-Merck, F0392), 1% Penycillin/Streptavidin, alanine (430 µM), asparagine (50 µM), aspartic acid (20 µM), glutamic acid (80 µM), proline (200 µM) with = Complete DMEM or without serine (150 µM) and Glycine (300 µM) = -Ser/Gly DMEM (Supplementary table 1).

Construct and viral transduction. The following constructs were used for knockdown experiments: For human protein: pLKO.1_Puro shMDM2 (Sigma-Aldrich mission clone #3377), pLKO.1_Puro shATF4 (Sigma-Aldrich mission clone #13577), pLKO.1_Puro shIL-6 (Sigma-Aldrich mission clones #59205, #59206, #59207).

For Murine protein: pLKO.1_Puro shMDM2 (Sigma-Aldrich mission clones #302276), pLKO.1_Puro shATF4 (Sigma-Aldrich mission clones #301646, #301731, #71724), pLKO.1_Puro shPHGDH (Sigma-Aldrich mission clones #41624, #41627, #41625), pLKO.1_Puro shPSAT1 (Sigma-Aldrich mission clones #120417, #120420, #120421), pLKO.1_Puro shPSPH (Sigma-Aldrich mission clones #81493, #81494, #81497), pLKO.1_Puro shIL6-Rα (Sigma-Aldrich mission clones #375089, #68293, #305257). Lentivirus was prepared by co-transfection of 293 T cells with shRNA of interest along with packaging plasmids pMD2.G (AddGene, cat. 12259), psPAX2 (AddGene, cat. 12260) and Lipofectamine 2000 transfection reagent (Invitrogen, cat. 15338). Lentivirus-containing media was collected from plates at 48 h post-transfection, filtered using a 0.45µm filter, and stored at −80 °C. For viral transduction, cells were incubated with lentivirus-containing medium and 8 µg/mL polybrene for 6 h. Cells were allowed to recover for another 48 h before selection with puromycin. All experiments were performed with cells that survived puromycin selection and displayed knockdown of MDM2, ATF4, PHGDH, PSAT1, IL6 and IL6Rα as assayed by western blot.

C2C12 cells were transfected using Lipofectamine 2000 to express Serine synthesis reporter gene: *Phgdh* (C2C12 Luc-*Phgdh*) or *Psat1* (C2C12 Luc-*Psat1*). Transduced myoblasts cells were selected with Hygromycine (2 µg/ml, Invitrogen) for 72 h.

Proliferation Assay. C2C12 cells were conditioned to produce serine by seeding them at 8 K/insert (Starsted, #833930040), 5 h later inserts were transferred to a 6 well-plate containing 80 K of IB115-GFP, and incubated for 72 h. IB115-GFP were seeded in DMEM 10%FBS at 20 K/well in 6 wells plate (Falcon #353046) after 5 hours plates and insert were washed 2 times with PBS and complete or -Ser/Gly medium was added to each well. LPS cell proliferation was monitored in real-time for 3 to 6 days using the Incucyte S3 Live-Cell Analysis system, whole-well module. The confluence value of each well was automatically monitored by the Incucyte system for 3-6 days and expressed as a value representing the relative confluence area. Normalized Confluence was calculated by dividing the Confluence for each time point by the original Confluence. Effects of serine and Glycine deprivation on cell proliferation were confirmed by manual counting after trypan blue exclusion performed at the end of the experiments. For crystal violet colorimetric assays, at the indicated time points, media was aspirated and cells were washed once with 1 ml (6-well) or 0.5 ml (12-well) of DPBS. Cells were then fixed using 4% paraformaldehyde (thermofisher) for 10 min. Cells were washed again using DBPS. A solution of 0.5% crystal violet (Sigma-Aldrich, catalog # C6158) in DPBS was added down the sides of each well. Cells were incubated with crystal violet for 20 min with gentle rocking. Crystal violet solutions were aspirated and then cells were washed twice with sterile water. Following water aspiration, plates were inverted and dried for 1 hour. Quantification of crystal violet staining was performed by adding an equivalent volume of 10% acetic acid, incubating plates at room temperature for 5 min with gentle rocking and then reading absorbance at OD 570 nm.

Co-culture assay. C2C12 and LPS-cells (IB111, IB115), were seeded in 6-well plate with a ratio 1:2: 90 K C2C12, 180 K LPS-cells, in

https://doi.org/10.1038/s41467-024-51827-3

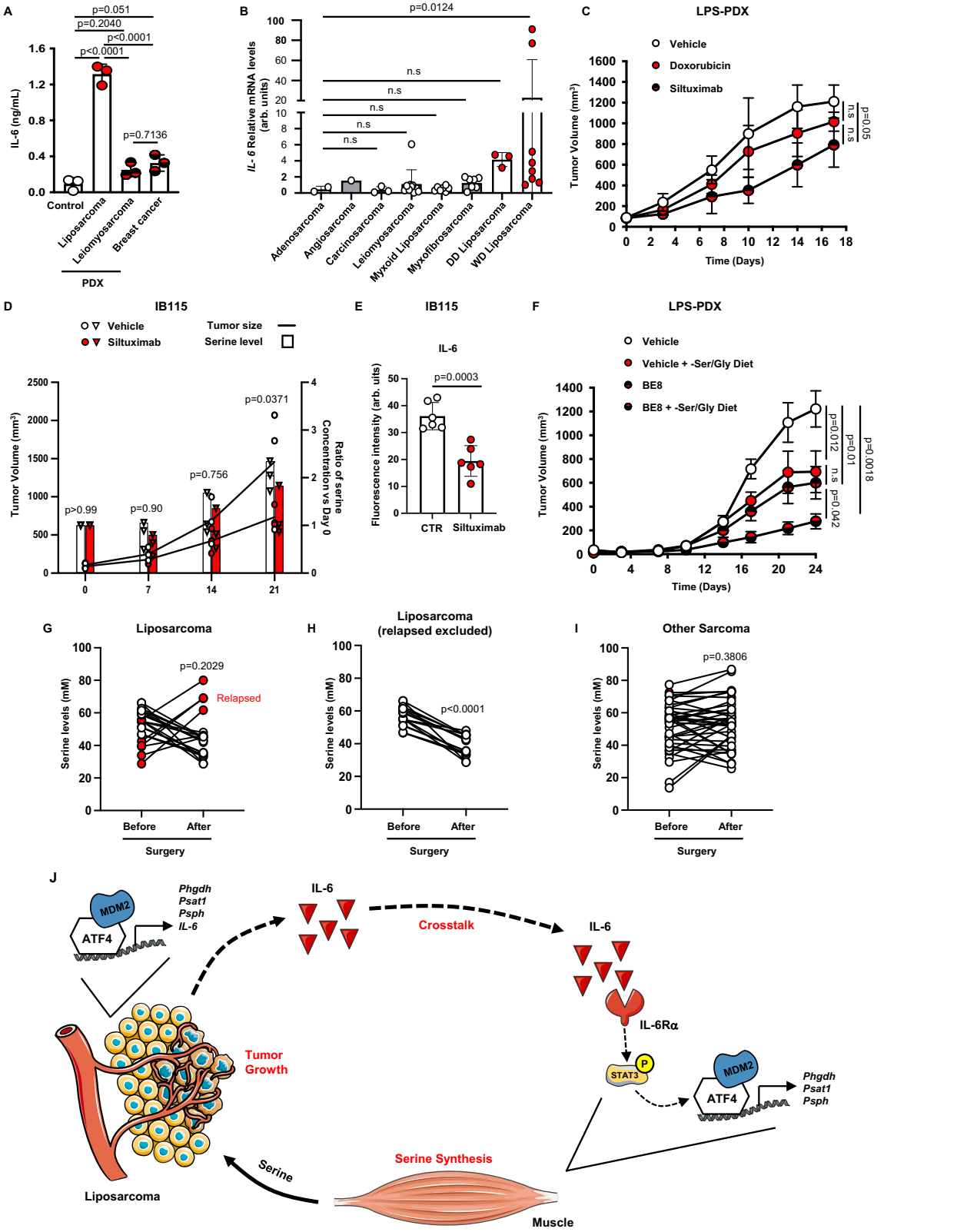

2 ml DMEM medium, for 48 h. Similarly, cells (ratio 1:2) were cultivated separately using an insert. These experiments were also carried out using the shRNA-mediated depleted cells or with the addition of drugs. Cells in culture alone or co-culture with LPS-cells were treated or not with a blocking anti-IL-6 antibody (Elsilimomab (BE8), mAB 1339 (humanized BE8), Siltuximab, 10 µg/ml), an anti-IL-6 receptor (Tocilizumab (20 µg/ml)) or inhibitor (Bazedoxifène, 100 nM), or STAT3 inhibitors such as C188-9 and Stattic (10 nM).

Conditioned media (CM) assay. Myoblasts were seeded at 100 K/well in a 6-well plate. About 30 h after, the medium was changed, and 200 µl of LPS-cells conditioned media (quantity corresponding to an IL-6 concentration finale of 150–300 pg/ml) + 1.8 mL of DMEM or 2 mL

Fig. 5 | IL-6 inhibition as a new therapy in liposarcoma. A IL6 concentration (ng/ml), measured by ELISA. Control mice were compared to Liposarcoma, Leiomyosarcoma and Breast cancer PDX Mice. ($n = 3$ independent experiments). **B** Real-time qPCR analysis of *IL-6* mRNA level in frozen patient samples from different sarcoma subtypes (Adenocarcinoma $n = 2$, angiosarcoma $n = 1$, carcinosarcoma $n = 3$, leiomyosarcoma $n = 10$, myxoid-liposarcoma $n = 7$, myxofibrosarcoma $n = 7$, WDLPS $n = 9$, DD-LPS $n = 3$). **C** Tumor growth curves from patient liposarcoma subcutaneously implanted in nude mice treated or not with Siltuximab (10 mg/kg) or doxorubicine (2 mg/kg) by IP twice weekly. Tumor volume was assessed at the indicated timepoints using caliper measurements. ($n = 6$ animals/group). **D** Tumor growth curves from IB115 LPS cell lines subcutaneously implanted in nude mice treated or not with Siltuximab (10 mg/kg) by IV daily. Tumor volume was assessed at the indicated timepoints using caliper measurements ($n = 3$ animals/group). **E**, IL-6 expression assessed by immunofluorescence performed from IB115 LPS tumors treated or not with Siltuximab (10 mg/kg) by IP twice weekly. ($n = 6$ samples/group). **F**, Tumor growth curves from patient liposarcoma tumor subcutaneously implanted in nude mice, fed a normal or a no Serine/Glycine diet and treated or not with anti-IL-6, BE8 (10 mg/kg) by IP twice weekly after tumor volume reached approximately 150mm^3. Tumor volume was assessed at the indicated timepoints using caliper measurements ($n = 3$ experimental replicates with 6 animals/group). Quantification of serum Serine levels (mM) from Liposarcoma patients ($n = 21$ samples/group) **G**, from Liposarcoma patients (relapsed patients excluded); ($n = 15$ samples/group) **H** before and 30 days after surgery, using liquid chromatography-high resolution mass spectrometry (LC/HRMS). Relapsed patients were highlighted in red. **I** Quantification of serum Serine levels (mM) from Sarcoma patients before and 30 days after surgery, using liquid chromatography-high resolution mass spectrometry (LC/HRMS). ($n = 38$ samples/group). **J** Schematic representing the crosstalk between liposarcoma and muscle initiated through IL-6/STAT3 pathway activation. Data are shown as means ± SEM and three or more independent experiments were performed. Statistical tests were all adjusted for multiple comparisons and included two-tailed unpaired t-test for (e), one-way (a, b), two-way analysis of variance (ANOVA) (c, d, f) and two-tailed paired and non-parametric Wilcoxon test for g, h and i. *$P < 0.05$, **$P < 0.01$, ***<0.001, n.s non-significant. Source data are provided as a Source Data file.

of DMEM was added to each well. Cells were collected after 16 hours. IL6 recombinant experiments were done using the same experimental setting but by adding 50 pg/ml of Human IL-6 recombinant proteins instead of CM on C2C12 cells.

RNA extraction and quantitative PCR. Total mRNAs were prepared using TriZol Reagent (Invitrogen). cDNAs were synthesized from 1 μg of total RNA using SuperScript III Reverse Transcriptase (Invitrogen). Real-time quantitative PCRs were performed on a LightCycler 480 SW 1.5 apparatus (Roche) using the Platinum Taq DNA polymerase (Invitrogen) and a SYBR Green mix containing 3 mM MgCl2 and 30 μM of each dNTP using the following amplification procedure: 45 cycles of 95 °C for 4 s, 60 °C for 10 s, and 72 °C for 15 s. The relative mRNA copy number was calculated using Ct value and normalized to at 2 or 3 housekeeping genes. Sequence of primers used for qPCR are listed in Supplementary table 4.

Immunoblotting. Protein extracts were subjected to SDS-PAGE and immunoblotted with the following primary antibodies: Mouse monoclonal: TBP (Santa Cruz, sc-56795), β-tubulin (Sigma-Aldrich, T6199), MDM2 (clones 4B11, and 2A10, Cell signaling and Millipore), STAT3 (Cell Signaling, 9139). Rabbit polyclonal: p-STAT3 (Cell signaling, 9145 T), PHGDH (Cell Signaling, 13428), PSAT1 (Sigma, SAB2108040), PSPH (Santa Cruz, sc-365183), HSP90 (Cell Signaling, 4877). All antibodies were used at the dilution 1/1000. The proteins of interest were then detected either by incubation with horseradish peroxidase-conjugated anti-mouse and anti-rabbit IgG (Cell Signaling) secondary antibodies and revealed using the Pierce ECL Western Blotting Substrate or the SuperSignal West Femto Maximum Sensitivity Substrate (Thermo Fisher Scientific), or 488-, 680- fluorescent Antibodies (Li-Cor). Quantification of immunoblots was performed by densitometric analysis of the corresponding bands using ImageStudio and ImageJ software.

Annexin V-7AAD apoptosis assay. Cell death was determined using the FITC–Annexin V, 7AAD Kit (catalog no. 35-6410) from Cytek according to the manufacturer's instructions. Briefly, C2C12 and IB115 cells were cultivated separately (using an insert) in triplicate in 6-well plates with a ratio 1:2, in 2 mL DMEM medium for three days. 24 h after plating, cells were treated or not for 48 h with either BE8, Siltuximab, or vehicle (water). Flow cytometry was performed using the Gallios flow cytometer (Beckman Coulter). The percentage of cells in early apoptosis (Annexin V-positive and 7AAD-negative) and in late apoptosis or necrosis (Annexin V- and 7AAD-positive) was calculated using FlowJo version 10.8.1 For Windows (Tree Star Inc).

Fluorescent in situ hybridization. Cells were seeded in 2 wells, Labteck 2 days before the experiment. Cells are fixed with 4% PFA for 10 min, washed 2 times with PBS, permeabilized for 10 min with Triton 0.1% and washed again 2 times. Slides are dehydrated in successive 2 min ethanol baths (70%, 80%, and 100%) and dried for 20 min. Probes are applied to each well, and Fixogum is used to sealed slide and slate before a 20 h incubation in a Neobrite 6.0 (80 °C for 5 min and 20 h at 37 °C). Remove the glue then wash slides for 2 min in wash buffer I (2x SCC, 0.1% tween20), another 10 min in wash buffer II at 65 °C and finally 3 minutes twice in wash buffer I (0.4x SSC + 0.1% tween20). Slides are dehydrated again in ethanol baths and sealed with a mounting medium before reading them using a Zeiss Axioimager M2 Apotome2.

Histological analyses, immunofluorescence and immunohistochemistry. Tissues biopsies were collected and fixed 24 h in neutral buffered formalin 10%, dehydrated, and embedded in paraffin. Paraffin-embedded tissue was cut into 3-μm-thick sections, mounted on slides, then dried at 37 °C overnight. Immunostaining was performed on 3 μm sections using appropriated primary antibody: anti-IL-6 antibody (ab6672 abcam 1:400), anti-Ki67 (M3064 spring bioscience 1:250), anti-caspase3 (9661S cell signaling 1:4000).

Immunohistochemistry was performed, as described previously (Rahmanzadeh, G. et al 2007), on a VENTANA Discovery Ultra automated staining instrument (Ventana Medical Systems), using VENTANA reagents, according to the manufacturer's instructions. Briefly, slides were de-paraffinized. Then epitope retrieval was performed with CC2 solution (cat# 950-123) at high temperature (eg, 91 °C) for Caspase3 and with CC1 solution (cat# 950-124) for Ki67, for a period of time that is suitable for each specific antibody. Endogenous peroxidase was blocked with Discovery Inhibitor (cat# 760-4840). Casp3 antibodies were incubated 32 min at 37 °C and Ki67 antibodies for 60 min at 37 °C. Signal enhancement was performed using the Omni-Map anti-rabbit detection kit (cat# 05266548001) for 16 min. Slides were incubated with DAB (cat# 05266645001) then counterstained with hematoxylin II (cat# 790-2208) for 8 min, followed by Bluing reagent (cat# 760-2037) for 4 min. Slides were then dehydrated with Leica autostainer and coverslipped with Pertex mounting medium with CTM6 coverslipper (Microm). For IL-6 immunofluorescence, slides were de-paraffinized, rehydrated and the epitope retrieval was performed by boiling slides for 30 min in citrate ph6 buffer (Diapath T0050). After cooling down to room temperature, slides were blocked in 3% BSA for 1 h. Next, tissue slides were incubated with the primary antibody at 4 °C overnight. Then, Alexa594-coupled donkey anti-rabbit secondary antibody (A21207 Invitrogen 1:500) was added onto these slides for 45 min at room temperature and mounted with fluoroshield DAPI (F6057 sigma).

Analyses of immunochemistry slides were performed with QuPath and immunofluorescence slides with ImageJ.

IL-6 concentration Assay. IL-6 concentration in the supernatant of the different cancer cell lines, and mice Serum was measured by an immunoassay (*Murine or* Human IL-6 Standard TMB ELISA Development Kit Catalog Number: 900-T50) following the manufacturer's instructions. Cells supernatant was collected after 48 h of culture, and centrifuged at 200 *g*. Mice serum was prepared by collecting 500 µL to 1 ml of blood from mice upon sacrifice in anticoagulant (Heparin 10 µl/tube, 5000UI/ml). Mice blood was then centrifuged at 800 g for 20 min without the brakes, serum was then transferred to a vial, and stored frozen prior to analysis.

XG-6 viability assay. The IL-6-dependent cell line XG-6 was cultured at a concentration of 1, 5* 10^5 cells/ml in RPMI medium in presence of recombinant IL-6 (control, 2 ng/ml) or supernatant from two different cell lines (MCF7 breast cancer cells or IB115 liposarcoma cells) for 72 hours. The number of XG-6 cells (AU) was measured by manual counting after trypan blue exclusion and CellTiter-Glo® Luminescent Cell Viability Assay (Promega, # G7570)

ChIP experiment assay. Cells were collected and processed as previously described by Riscal et al. (2016). The Immunoprecipitation was performed using an anti-MDM2 (Santa Cruz, sc-813), anti-ATF4 (Cell signaling, 11815S), or a polyclonal rabbit IgG (Cell Signaling, 2729S) that serves as a control. Samples were than analyzed by qPCR using primers specific to IL-6 and TRIB3.

High Performance Liquide Chromatography. Mice and patients' serum samples were prepared directly upon collection as follow: blood was collected in anticoagulant (Heparin, EDTA coated collection tubes), then centrifuged at 800 g for 20 min, without the brakes. 30% acid salicylic was added to the samples and centrifuged again, supernatant was transferred to a vial, and store frozen prior analysis. The measurement was performed using an Agilent HPLC and data were analyzed using R studio.

Instrumentation and conditions LC/MSMS analysis

Mice and patients' serum samples was prepared directly upon collection as follows: blood was collected in anticoagulant (Heparin, EDTA coated collection tubes), then centrifuged at 800 g for 20 min, without the brakes. 30% acid salicylic was added to the samples and centrifuged again, the supernatant was transferred to a vial, and store frozen prior analysis.

UHPLC analysis

The chromatographic apparatus consisted of Nexera X2 UHPLC system (Shimadzu, Marne la Vallée, France) equipped with a binary pump, solvent degasser, and thermostatted column compartment. A Atlantis Premier BEH C18 AX (1.7 µm; 2, 1 × 100 mm) (Waters) was used for separation. Mobile phase A is waters with 0.1 % of formic acid, and eluent B is acetonitrile with 0.1% of acid formic too. The gradient used is reported in the supplementary table 5. The flow rate was 0, 4 mL/min.

MS/MS detection

MS/MS experiments were carried out using the Shimadzu UHPLC system described above coupled to a Shimadzu LCMS-8050 triple quadrupole mass spectrometer using the multiple reaction

monitoring (MRM) technique operating in positif mode. The mass parameters used for experiments: Nebulizing Gas Flow at 3 L/min; Heating Gas Flow at 10 L/min, Interface Temperature at 300 °C, the Dl Temperature is at 250 °C, the Heat Block Temperature is at 400 °C and the drying Gas flow is at 10 L/min. All transitions and the dwell times were optimized by LabsSolution Main For each MRM transition; optimal CE values were chosen for each compound to obtain the most characteristic fragments (supplementary table 6). The data analysis were performed by LabSolutions Insight LCMS. We use 13 C serine-like internal standard.

In vivo experiments. All procedures were approved by the ethic committee for animal warfare of the region Languedoc Roussillon (Comité d'Ethique en Expérimentation Animal Languedoc Roussillon) which is an accredited institution of the French "MINISTERE DE L'ENSEIGNEMENT SUPERIEUR, DE LA RECHERCHE ET DE L'INNOVATION" (agreement numbers # E 34-172-27 and # 2021011115238381-#28923). Animal housing and euthanasia were performed in accordance with the 3 R rule and with recommendations of the Guide for the Care and Use of Laboratory Animals.

All the experiments were processed with Female CR ATHYMIC HO MOUSE (490CRATHHO, Charles River) aged to 8 weeks. Xenograft models are generally females. Sex was not considered in the study design.

Mice liposarcoma PDX models were established in collaboration with the surgical and pathology departments of the "Institut du Cancer de Montpellier" (ICM) by inserting a human tumor fragment of approximately 40 mm^3 subcutaneously on 8-week-old Nude mice. Volumetric measurements of xenografted tumors were performed every 3 days by the same person using a manual caliper (volume = length × $width^2$/2). For all PDX models used in this study (liposarcomas or other sarcomas), tumors reached 100 mm^3 in the 3 to 4 weeks after ungrafting and the endpoint of 1000 mm^3 is reached in 6 to 8 weeks. All animals were euthanized when the first animal reached the ethical endpoint (volume = 1000 cm^3 or ulceration). Before the experiment, animals were fed with chow diet (Safe A04). During our experiments, mice were either fed with a control diet (called Amino Acid diet; TD 99366 Harlan ENVIGO) or a test diet (Harlan Envigo, TD 130775: diet lacking serine and glycine) during 4 weeks. The diets had equal caloric value (3.9 kCal/g), an equal amount of total amino acids (179.6 g/kg), and were in the form of kibbles for mice. Total food intake was controlled to be identical in all experimental groups. Mice are housed in individually ventilated caging (IVC) systems with a 12 light/12 dark cycle, an ambient temperature of 22+/-1 °C and a humidity of 35 to 50%, in a pathogen-free barrier facility in accordance with the regional ethics committee for animal warfare (n°CEEA-LR-12067). Anti-IL-6 antibody (BE8 and Siltuximab), SP141, and doxorubicin were administered by IP injection at the dose of 10 mg/kg twice a week for 3 weeks, 40 mg/kg weekly, and 2 mg/kg weekly respectively.

13 C stable isotope tracing experiments. Measurement of 13C incorporation in intracellular and extracellular amino acids upon incubation with 13C-labeled glucose was separated on a PFP column (150 × 2.1 mm i.d., particle size 5 µm; Supelco Bellefonte, PEN, USA). Solvent A was 0.1% formic acid in H20 and solvent B was 0.1% formic acid in acetonitrile at a flow rate of 250 µL/min. The gradient was adapted from the method used by Boudah et al.[48] Solvent B was varied as follows: 0 min: 2%, 2 min: 2%, 10 min: 5%, 16 min: 35%, 20 min: 100% and 24 min: 100%. The column was then equilibrated for 6 min at the initial conditions before the next sample was analyzed. The volume of injection was 5 µL. High-resolution experiments were performed with a Vanquish HPLC system coupled to an Orbitrap Qexactive+ mass spectrometer (Thermo Fisher Scientific, Waltham, MA, USA) equipped with a heated electrospray ionization probe. MS analyses were performed in positive FTMS mode at a resolution of 70 000 (at 400 m/z) in full-scan mode, with the following source parameters: the capillary temperature was 320 °C, the source heater temperature, 300 °C, the sheath gas flow rate, 40 a.u. (arbitrary unit), the auxiliary gas flow rate, 10 a.u., the S-Lens RF level, 40%, and the source voltage, 5 kV. Metabolite isotopologs were determined by extracting their exact mass with a tolerance of 5 ppm.

Statistics and reproducibility. Data collection and statistics were performed in Microsoft Excel and GraphPad Prism (Version 10). All in vitro experiments and assays were performed in three or more independent biological replicates unless specified. All in vivo

experiments were performed on at least 5 animals for each group unless specified. For mouse xenograft essays, the size of the experimental groups was calculated on the basis of previous experiments to reach a statistical test power of 0.80 and a significance of 0.05. Groups of mice were randomized by the size of the tumor at the beginning of the experiment. Experiments were performed in accordance with protocols approved by the French Council of Animal Care guidelines and national ethical guidelines of the Institut National de la Santé et de la Recherche Médicale (INSERM) Animal Care Committee. The researchers were blinded for the measurement of tumor sizes in vivo and for the analysis of in vitro results. Statistical tests were all adjusted for multiple comparisons with unpaired t-test, one-way or two-way analysis of variance (ANOVA) and paired non-parametric Mann-Whitney. $^{*}P < 0.05$, $^{**}P < 0.01$, $^{***}<0.001$, n.s non-significant were applied.

Reporting summary

Further information on research design is available in the Nature Portfolio Reporting Summary linked to this article.

Data availability

Correspondence and requests for materials should be addressed to Laetitia K Linares or Romain Riscal. Source data are provided with this paper. RNAseq data used for this study is available from GSO with the accession code GSE221494 [https://www.ncbi.nlm.nih.gov/geo/query/acc.cgi?acc=GSE221492][49]. Metabolic data are available in metabolights as MTBLS10199. The remaining data used for this study are present in the Article, Supplementary and Source Data files. Source data are provided with this paper.

References

1. Mastrangelo, G. et al. Incidence of soft tissue sarcoma and beyond: a population-based prospective study in 3 European regions. *Cancer* **118**, 5339–5348 (2012).
2. Verweij, J. & Baker, L. H. Future treatment of soft tissue sarcomas will be driven by histological subtype and molecular aberrations. *Eur. J. Cancer Oxf. Engl. 1990* **46**, 863–868 (2010).
3. Ducimetière, F. et al. Incidence of sarcoma histotypes and molecular subtypes in a prospective epidemiological study with central pathology review and molecular testing. *PloS One* **6**, e20294 (2011).
4. ESMO/European Sarcoma Network Working Group Soft tissue and visceral sarcomas: ESMO Clinical Practice Guidelines for diagnosis, treatment and follow-up. *Ann. Oncol. J. Eur. Soc. Med. Oncol.* **25**, iii102–iii112 (2014).
5. Singer, S., Antonescu, C. R., Riedel, E. & Brennan, M. F. Histologic subtype and margin of resection predict pattern of recurrence and survival for Retroperitoneal Liposarcoma. *Ann. Surg.* **238**, 358–371 (2003).
6. Jones, R. L., Fisher, C., Al-Muderis, O. & Judson, I. R. Differential sensitivity of liposarcoma subtypes to chemotherapy. *Eur. J. Cancer Oxf. Engl. 1990* **41**, 2853–2860 (2005).
7. van der Graaf, W. T. A. et al. Pazopanib for metastatic soft-tissue sarcoma (PALETTE): a randomised, double-blind, placebo-controlled phase 3 trial. *Lancet Lond. Engl.* **379**, 1879–1886 (2012).
8. Coindre, J.-M., Pédeutour, F. & Aurias, A. Well-differentiated and dedifferentiated liposarcomas. *Virchows Arch.* **456**, 167–179 (2010).
9. Lee, A. T. J., Thway, K., Huang, P. H. & Jones, R. L. Clinical and Molecular Spectrum of Liposarcoma. *J. Clin. Oncol.* **36**, 151–159 (2018).
10. Crago, A. M. & Singer, S. Clinical and molecular approaches to well differentiated and dedifferentiated liposarcoma. *Curr. Opin. Oncol.* **23**, 373–378 (2011).
11. Lokka, S. et al. Challenging dedifferentiated liposarcoma identified by MDM2-amplification, a report of two cases. *BMC Clin. Pathol.* **14**, 36 (2014).
12. Hou, H., Sun, D. & Zhang, X. The role of MDM2 amplification and overexpression in therapeutic resistance of malignant tumors. *Cancer Cell Int.* **19**, 216 (2019).
13. Marine, J.-C. & Lozano, G. Mdm2-mediated ubiquitylation: p53 and beyond. *Cell Death Differ.* **17**, 93–102 (2010).
14. Montes de Oca Luna, R., Wagner, D. S. & Lozano, G. Rescue of early embryonic lethality in mdm2-deficient mice by deletion of p53. *Nature* **378**, 203–206 (1995).
15. Jones, S. N., Roe, A. E., Donehower, L. A. & Bradley, A. Rescue of embryonic lethality in Mdm2-deficient mice by absence of p53. *Nature* **378**, 206–208 (1995).
16. Bouska, A. & Eischen, C. M. Mdm2 affects genome stability independent of p53. *Cancer Res* **69**, 1697–1701 (2009).
17. Léveillard, T. & Wasylyk, B. The MDM2 C-terminal region binds to TAFII250 and is required for MDM2 regulation of the cyclin A promoter. *J. Biol. Chem.* **272**, 30651–30661 (1997).
18. Bohlman, S. & Manfredi, J. J. p53-independent effects of Mdm2. *Subcell. Biochem.* **85**, 235–246 (2014).
19. Wienken, M. et al. MDM2 associates with polycomb repressor Complex 2 and enhances stemness-promoting Chromatin modifications independent of p53. *Mol. Cell* **61**, 68–83 (2016).
20. Klusmann, I. et al. Chromatin modifiers Mdm2 and RNF2 prevent RNA:DNA hybrids that impair DNA replication. *Proc. Natl Acad. Sci. USA.* **115**, E11311–E11320 (2018).
21. Feeley, K. P., Adams, C. M., Mitra, R. & Eischen, C. M. Mdm2 is required for survival and growth of p53-deficient cancer cells. *Cancer Res* **77**, 3823–3833 (2017).
22. Riscal, R. et al. Chromatin-bound MDM2 regulates serine metabolism and redox homeostasis independently of p53. *Mol. Cell* **62**, 890–902 (2016).
23. Cissé, M. Y. et al. Targeting MDM2-dependent serine metabolism as a therapeutic strategy for liposarcoma. *Sci. Transl. Med.* **12**, eaay2163 (2020).
24. Ray-Coquard, I. et al. Effect of the MDM2 antagonist RG7112 on the P53 pathway in patients with MDM2-amplified, well-differentiated or dedifferentiated liposarcoma: an exploratory proof-of-mechanism study. *Lancet Oncol.* **13**, 1133–1140 (2012).
25. Zhu, H. et al. Targeting p53–MDM2 interaction by small-molecule inhibitors: learning from MDM2 inhibitors in clinical trials. *J. Hematol. Oncol.* **15**, 91 (2022).
26. LoRusso, P. et al. The MDM2–p53 Antagonist Brigimadlin (BI 907828) in patients with advanced or metastatic solid tumors: results of a phase ia, first-in-human, dose-escalation study. *Cancer Discov.* **13**, 1802–1813 (2023).
27. Tajan, M. et al. Serine synthesis pathway inhibition cooperates with dietary serine and glycine limitation for cancer therapy. *Nat. Commun.* **12**, 366 (2021).
28. Wu, P. et al. Adaptive mechanisms of tumor therapy resistance driven by tumor microenvironment. *Front. Cell Dev. Biol.* **9**, 641469 (2021).
29. Chang, C.-H. et al. Metabolic competition in the tumor microenvironment is a driver of cancer progression. *Cell* **162**, 1229–1241 (2015).
30. Geiger, R. et al. L-Arginine modulates T cell metabolism and enhances survival and anti-tumor activity. *Cell* **167**, 829–842.e13 (2016).
31. Fletcher, M. et al. l-Arginine depletion blunts antitumor T-cell responses by inducing myeloid-derived suppressor cells. *Cancer Res* **75**, 275–283 (2015).
32. Shang, M. et al. Macrophage-derived glutamine boosts satellite cells and muscle regeneration. *Nature* **587**, 626–631 (2020).
33. Maddocks, O. D. K. et al. Serine starvation induces stress and p53-dependent metabolic remodelling in cancer cells. *Nature* **493**, 542–546 (2013).

34. Holeček, M. Serine metabolism in health and disease and as a conditionally essential amino acid. *Nutrients* **14**, 1987 (2022).
35. Ding, J. et al. The histone H3 methyltransferase G9A epigenetically activates the serine-glycine synthesis pathway to sustain cancer cell survival and proliferation. *Cell Metab.* **18**, 896–907 (2013).
36. Zhao, E. et al. KDM4C and ATF4 cooperate in transcriptional control of amino acid metabolism. *Cell Rep.* **14**, 506–519 (2016).
37. Püschel, F. et al. Starvation and antimetabolic therapy promote cytokine release and recruitment of immune cells. *Proc. Natl Acad. Sci.* **117**, 9932–9941 (2020).
38. Iwasaki, Y. et al. Activating transcription factor 4 links metabolic stress to interleukin-6 expression in macrophages. *Diabetes* **63**, 152–161 (2014).
39. Brighenti, E. et al. Interleukin 6 downregulates p53 expression and activity by stimulating ribosome biogenesis: a new pathway connecting inflammation to cancer. *Oncogene* **33**, 4396–4406 (2014).
40. Mauer, J., Denson, J. L. & Brüning, J. C. Versatile functions for IL-6 in metabolism and cancer. *Trends Immunol.* **36**, 92–101 (2015).
41. Ni, C.-W., Hsieh, H.-J., Chao, Y.-J. & Wang, D. L. Interleukin-6-induced JAK2/STAT3 signaling pathway in endothelial cells is suppressed by hemodynamic flow. *Am. J. Physiol. Cell Physiol.* **287**, C771–C780 (2004).
42. Chen, Y. et al. Activating transcription factor 4 mediates hyperglycaemia-induced endothelial inflammation and retinal vascular leakage through activation of STAT3 in a mouse model of type 1 diabetes. *Diabetologia* **55**, 2533–2545 (2012).
43. Italiano, A., Garbay, D., Cioffi, A., Maki, R. G. & Bui, B. Advanced pleomorphic liposarcomas: clinical outcome and impact of chemotherapy. *Ann. Oncol. J. Eur. Soc. Med. Oncol.* **23**, 2205–2206 (2012).
44. Mullarky, E., Mattaini, K. R., Vander Heiden, M. G., Cantley, L. C. & Locasale, J. W. PHGDH amplification and altered glucose metabolism in human melanoma. *Pigment Cell Melanoma Res.* **24**, 1112–1115 (2011).
45. Possemato, R. et al. Functional genomics reveal that the serine synthesis pathway is essential in breast cancer. *Nature* **476**, 346–350 (2011).
46. Rinaldi, G. et al. In vivo evidence for serine biosynthesis-defined sensitivity of lung metastasis, but not of primary breast tumors, to mTORC1 inhibition. *Mol. Cell* S1097276520308273 https://doi.org/10.1016/j.molcel.2020.11.027 (2020).
47. Kang, S., Tanaka, T., Narazaki, M. & Kishimoto, T. Targeting Interleukin-6 signaling in clinic. *Immunity* **50**, 1007–1023 (2019).
48. Boudah, S. et al. Annotation of the human serum metabolome by coupling three liquid chromatography methods to high-resolution mass spectrometry. *J. Chromatogr. B* **966**, 34–47 (2014).
49. Gruel, N. et al. Cellular origin and clonal evolution of human dedifferentiated liposarcoma. *Nature Communications*. https://doi.org/10.1038/s41467-024-52067-1 (2024).

Acknowledgements

The authors would like to thank G. Gadea and C. Teyssier for their input and critical reading of the manuscript. We thank the CRB-ICM (BB-033-0059) for the tumor samples supplied for this study. We thank the IRCM's animal facility unit members (BioCampus RAM-PEFO, IRCM, Montpellier, France) for animal care and for in vivo studies. We thank the « Laboratoire de Mesures Physiques, Plateforme d'analyse chimique, Pôle Chimie Balard Recherche, Campus CNRS, Montpellier » for mass spectrometry experiment. We thank the "Réseau d'Histologie Expérimentale de Montpellier" - RHEM facility for histology techniques and expertise. RHEM facility is supported by SIRIC Montpellier Cancer Grant INCa_Inserm_DGOS_12553, REACT-EU (Recovery Assistance for Cohesion and the Territories of Europe), IBiSA, Ligue contre le cancer, the Occitanie/Pyrénées-Méditerranée and GIS FC3R whose funds are managed by Inserm. We also thank the imaging facility MRI, a member of the France-BioImaging national infrastructure supported by the French National Research Agency (ANR-10-INBS-04, «Investments for the future»)". We acknowledge the MetaToul (Metabolomics & Fluxomics Facilities, Toulouse, France) and its staff members for technical support and access to HRMS facilities. MetaToul is part of the national infrastructure MetaboHUB-ANR-11-INBS-0010. Finally, Illustrations were generated using Servier Medical Art.

Author contributions

G.M., R.R. and L.K.L., designed the studies, interpreted the data, and wrote the manuscript; G.M., A.A., B.R.M., J.P.R., R.R., B.F., L.G., M.L., S.J., C.S., G.P. and M.Y.C. performed the in vitro experiments; G.M., L.G., B.F. and L.K.L. contributed to the in vivo experiments. N.F. provided medical expertise. P.P. provided cell lines. N.G., C.Q., S.W and F.C. provided LPS characterization. M.H. and F.B. performed and analyzed ^{13}C glucose labelling experiments.

Funding

This research was supported by grants from the Fondation ARC (R19056FF/RAC19003FFA), the Ligue contre le Cancer (R19013FF/RAB19004FFA), INSERM (REC), Onward therapeutics (private support) and INCA (R18098FF/RPT1801FFA). G.M. was supported by a fellowship from the INSERM and Région Occitanie (R20061FF), J.P.R. was supported by "La Ligue Contre le Cancer", R.R was supported by the Fondation ARC, MYC and A.A. were supported by the university of Montpellier.

Competing interests

L.K.L., N.F., and G.M. are inventors on patent application no. 21 306099.9 submitted by ICM that covers "methods for the treatment of cancer". All other authors declare that they have no competing interests.

Additional information

Supplementary information The online version contains supplementary material available at https://doi.org/10.1038/s41467-024-51827-3.

Correspondence and requests for materials should be addressed to Romain Riscal or Laetitia K. Linares.

Peer review information *Nature Communications* thanks the anonymous reviewers for their contribution to the peer review of this work. A peer review file is available.